Seismic attenuation anisotropy and corresponding frequency versus azimuth (FVAz) attribute

Fangyu Li, University of Oklahoma; Huailai Zhou, Chengdu University of Technology;*
Bin Lyu, Jie Qi, and Kurt J. Marfurt, University of Oklahoma.

Summary

As globle resource plays, fractured reservoirs draw attentions from both the academy and industry. During the exploration and development, amplitude, traveltime, velocity, and attenuation anisotropies are valuable for both natural and hydraulic fractures. The fluid-flow effects and scattering effect can cause apparent attenuation, which makes attenuatation anisotropy attributes potientials in unconventional reservoir characterization. We derive the anisotripic attenuation expression, and then develop the asscoiated frequency versus azimuth (FVAz) attribute, which have been tested in synthetic example. In the field applications of unconventional resource plays, attenuation anisotropy and FVAz show promise and effectiveness in characterization of the fractured reservoirs.

Introduction

When propagating through the earth, seismic wave suffers energy loss as well as dispersion. Including scattering and intrinic attenuation, seismic attenuation anisotropy involves lithology, porosity, and fluid or gas saturation (Li et al., 2016). Aligned vertical fractures produces azimuthal variations in P-wave amplitude, travel-times, stacking velocity, attenuation variation, while the fluid flows in the fracures also affect seismic waveforms. Therefore, attenuation anisotropy study becomes a popular topic in theoretical, laboratory and applications (Schoenberg and Douma, 1988; MacBeth, 1999; Carione, 2000; Chichinina et al., 2007). Systematic effects have been demonstrated in surface seismic data shot over naturally fractured gas reservoirs (Lynn and Beckham, 1998). The predominant characteristic of all these observations is a greater P-wave attenuation in a propagation direction perpendicular to the fracture strike (Horne and MacBeth, 1997).

In this paper, we first provide a general review of attenuation and elastic stiffness matrix based attenuation anisotropy. Then, we derived the attenuation anisotropy equation, and from which we also get the frequency versus azimuth (FVAz) expression. After showing a synthetic exmaple of attenuation anisotropy, we apply the workflow on an unconventional survey to investiget the field situations.

Attenuation Coefficient and Phase Velocity

As the seismic attenuation effect has many different sources, and it is hard to distinguish them apart, the term "attenuation" used in the following paragraphs refers to the apprarent attenuation, which causes the overall effect of amplitude and frequency loss.

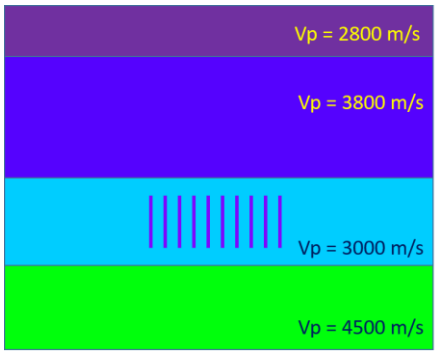

Figure 1: P-wave velocity model of the simple forward modeling. Because we want to simulate the fluid saturated aligned fractures, we set the velocity is low in the fractures.

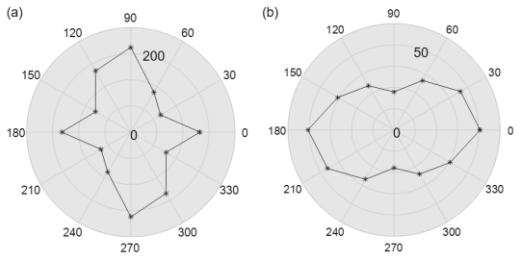

Figure 2: Azimuthal attenuation results from reflectors (a) below and (b) above the fractured layer of the model in Figure 1.

For a single propagating plane wave with no spherical divergence, the attenuation coefficient $\gamma(\omega)$ defines the seismic attenuation. For each angular frequency ω, the wave amplitude decays according to

$$A(\omega) = A_0(\omega) e^{-\gamma(\omega) r}, \tag{1}$$

where r is the pathlength and $A_0(\omega)$ is the initial amplitude. An alternative and much more appropriate measure of subsurface absorption is the Q (or specific attenuation) factor. This is defined as the fractional loss of energyin one cycle of wave motion, and is thus a positive number.

$$\gamma = \frac{\omega}{2vQ} = \frac{\omega}{2v} Q^{-1}, \tag{2}$$

where v is the phase velocity and Q values are normally quoted by the inverse.

For elastic anisotropy modeling, the wave properties arising from complex elastic constants can be determined using the same formulations as the elastic case by inserting the solution of displacement vector into the equation of motion. So, the complex phase slowness can be expressed as

$$\tilde{\mathbf{P}} = \mathbf{P}_R + i\mathbf{P}_I , \tag{3}$$

It follows that the wave must attenuate according to $e^{-\omega p_I r}$ for a distance r along each specific phase direction. The attenuation factor, $\gamma(\omega)$ is given by ωp_I and hence $Q^{-1}(\omega) = 2p_I / p_R$ from Equation (2) above. The velocity anisotropy is influenced through the real part, and the angle-dependent attenuation through the imaginary part.

Elastic Stiffnesses for Crack-related Anisotropy

A weak concentration of cracks or thin pores in an otherwise isotropic matrix generally weakens the rock, and hence reduces the background elastic stiffnesses, $\mathbf{C}_b$, by amounts proportional to the crack/fracture porosity ϕ_c. These elastic constants, with the resultant first order perturbation can be written in the generic form,

$$c = \begin{pmatrix} (\lambda+2\mu)(1-e_n) & \lambda(1-e_n) & \lambda(1-e_n) & 0 & 0 & 0 \\ \lambda(1-e_n) & (\lambda+2\mu)(1-\zeta^2 e_n) & \lambda(1-\zeta e_n) & 0 & 0 & 0 \\ \lambda(1-e_n) & \lambda(1-\zeta e_n) & (\lambda+2\mu)(1-\zeta^2 e_n) & 0 & 0 & 0 \\ 0 & 0 & 0 & \mu & 0 & 0 \\ 0 & 0 & 0 & 0 & \mu(1-e_t) & 0 \\ 0 & 0 & 0 & 0 & 0 & \mu(1-e_t) \end{pmatrix}, \tag{4}$$

where λ and μ are Lame constants, $\zeta = 1 - 2V_s^2 / V_p^2$, and e_n, e_t are the fracture indices.

For asymmetry planes, a formula for the general directional dependence may be determined by adapting Thomsen's (1986) weak anisotropy approximation for a transversely isotropic (TI) medium. Now, we introduce the phase velocity direction angle α, which depends on the azimuth ψ and the incidence θ, so $\cos\alpha = \cos\psi \sin\theta$.

When the fracture indices become complex $\tilde{e}_n = e_n^R + ie_n^I$, the weak parameters also have the complex format. Then, following Chichinina et al. (2007), the phase velocity equations for the P-waves can thus be rearranged for slowness

$$\tilde{p} = p_b \left(1 + \frac{\tilde{e}_t}{2} \eta \sin^2 2\alpha + \frac{\tilde{e}_n}{2} \left(1 - 2\eta \sin^2 \alpha \right)^2 \right), \tag{5}$$

where $\eta = V_s^2 / V_p^2$, and p_b is the background isotropic slowness. The imaginary part of the slowness is

$$p_I(\alpha) = p_b \frac{e_n^I}{2} \left(1 - 2\eta \sin^2 \alpha \right)^2 , \tag{6}$$

Which leads to

$$\gamma(\psi, \theta) = \omega p_b \frac{e_n^I}{2} \left(1 - 2\eta \sin^2 \alpha \right)^2 , \tag{7}$$

So

$$Q^{-1}(\psi, \theta) = \frac{e_n^I}{2} \left(1 - 2\eta \sin^2 \alpha \right)^2 , \tag{8}$$

Synthetic Example for Attenuation Anisotropy

Equation (8) clearly demonstrates that the attenuation should show anisotropic phenoumenon in TI medium. We build a simple synthetic model to measure the azimuthal variantions of attenuation. Figures 1 and 3 show two simple models without and with thin beds on the fracured layer.

From Figure 2(a) and 4(a), we find the expected results, that the attenuation is stronger when perpendicular to the fracures and weaker when parellel to the fractures. Note that, the results are not absolute ellipses, because Equation (8) considers the intrinsic attenuation from fractures, but they also produce scattering attenuations. Figures 2(b) and 4(b) show attenuation estimation results from the uppper boundaries of the fracured layer, and we can also observe anisotropic effects, which indicates the scattering attenuation also generate anisotropy but in a different strike. (Because the accuracy of the forward model, results from the synthetic examples don't match the equations perferctly, but the attenuation anisotropy can be clearly observed.)

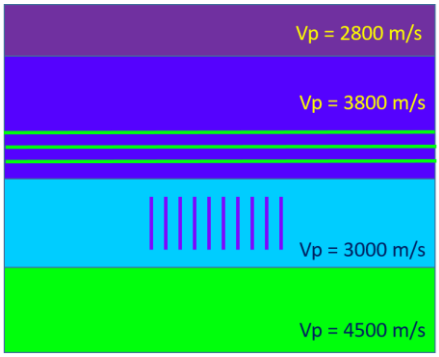

Figure 3: P-wave velocity model with thin beds on the fractured layer. Others are the same with the one in Figure 1.

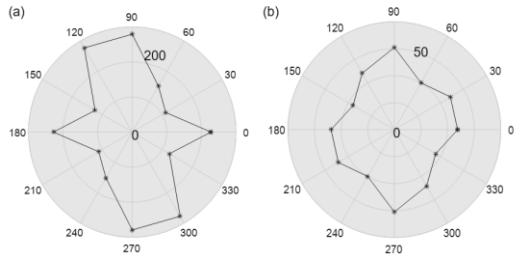

Figure 4: Azimuthal attenuation results from reflectors (a) below and (b) above the fractured layer of the model in Figure 3.

Frequency versus Azimuth (FVAz)

The central frequency of a signal is usually defined as

$$f_c = \frac{\int_0^\infty f \bullet \mathrm{S}(f)df}{\int_0^\infty \mathrm{S}(f)df}, \qquad (9)$$

where $\mathrm{S}(f)$ is the amplitude spectrum of signal $s(t)$.

From Equations (1), (8) and (9), we can conclude that as the attenuations from different azimuths are different, the spectra at different azimuths should be different, so the frequency attributes would show anisotropy.

Field Application

The Barnett Shale is a very important unconventional shale gas system in the Fort Worth Basin (FWB), Texas where it serves as a source rock, seal, and trap (Perez, 2009). The survey shown in Figure 5 was aquired after hydraulic fracturing using about 200 vertical and 200 horizontal wells (Thompson, 2010). No survey was acquired before the wells were drilled. By design, hydraullically induced fractures should have considerable gas charge. In the survey area, the relatively brittle Barnett Shale reservoir falls between the more ductile Marble Falls and Viola Limestones which form the frac barriers. A thin Forestburg Limestone separates the reservoir into Upper Barnett and Lower Barnett sections. The Viola and Forestburg formations are not producible and provide barriers to fault and fracture growth. Figure 5 shows the seismic data with the interpreted Upper Barnett shale and Lower Barnett shale, and the time structure of Lower Barnett shale with most negtive curvature attribute. Because the fracture scale is below the seismic resolution, curvature does not "see" any small scale fractures, it does measure strain, which is a component of natural fracture formation and thus zones of weakness and/or strength for subsequent stimulation. So, we can only infer the potential fracture densities, which should be larger along the natural faults and smaller at others positions.

Figure 6 shows the attenuation estimation results on full azimuth and different azimuths. It is clear that the seismic attenuation results show anisotropy. Based on Figure 5(c), we can have a simple understanding of the study area, and have the conceptions what are the fault plane strikes. So as expected, the attenuation attributes can be used to analyze the reservoir anisotropy. Figure 7 shows the FVAz results at different azimuths, which a have some correspondence with the results on Figure 6. Although in this application, because of the low resolution, FVAz results can't provide much useful information, when the signal-noise-ratio is low and attenuation results show a lot of interferences, FVAz will be very useful.

Conclusions

Seismic attenuation and frequency attributes are important poststack attributes. In order to figure out how to apply prestack attributes, we derive the attenuation anisotropy equations and FVAz. The synthetics and field application show they would be promising tools for unconventional reservoir characterizaiton.

Acknowledgement

We express our gratitude to the industry sponsors of the Attribute-Assisted Seismic Processing and Interpretation (AASPI) Consortium in the University of Oklahoma for their financial support. We thank the Key Lab of Earth Exploration and Information Techniques of Ministry of Education in Chengdu University of Technology of China for the partial financial support. We also thank colleagues in AASPI for their valuable input and suggestions. Special thanks to Devon Energy for the use of their seismic survey.

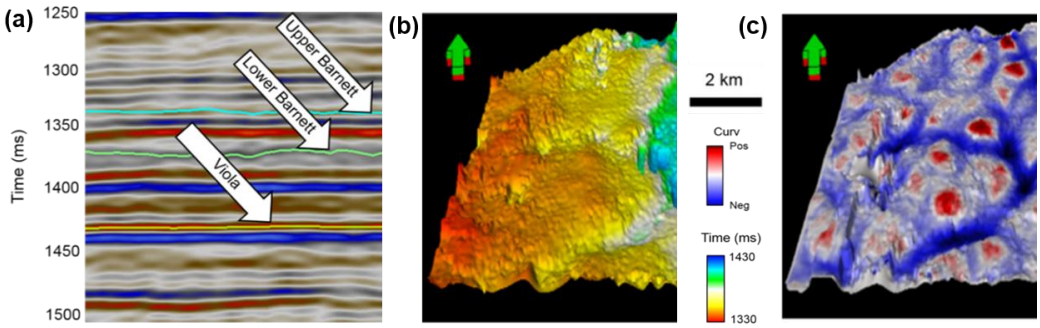

Figure 5: (a) Seismic data and interpreted horizon, (b) Time structure map of Lower Barnett shale, and (c) most negtive curvature attribute.

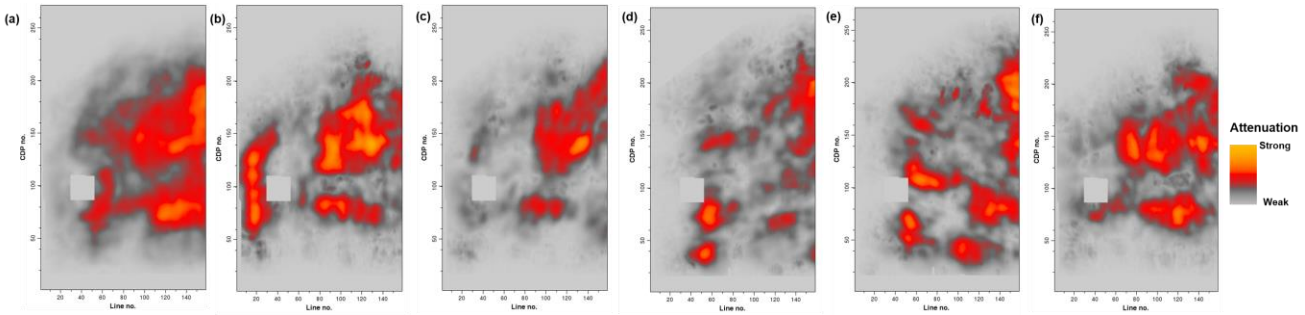

Figure 6: Attenuation anisotropy results from (a) full azimuth, (b) azimuth 0 degree, (c) azimuth 45 degree, (d) azimuth 90 degree, (e) azimuth 135 degree, and (f) azimuth 180 degree. The attenuation estimation results are different from each other, which shows the anisotropy.

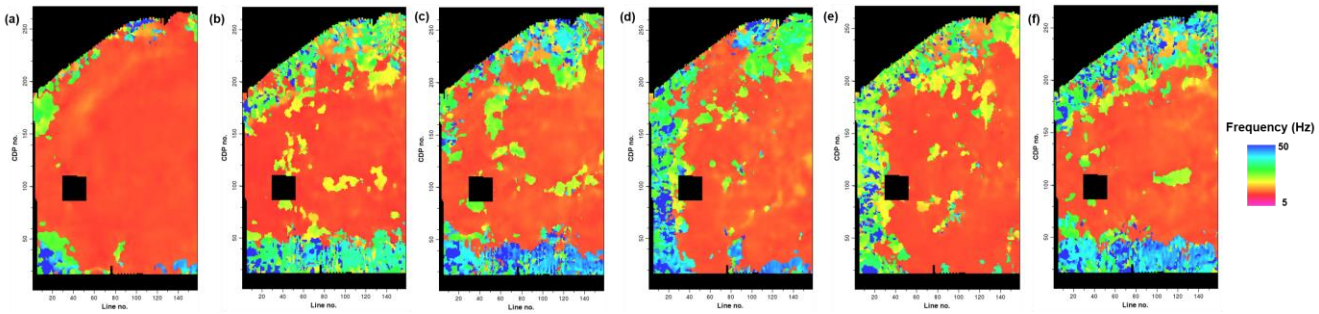

Figure 7: Frequency versus azimuth results from (a) full azimuth, (b) azimuth 0 degree, (c) azimuth 45 degree, (d) azimuth 90 degree, (e) azimuth 135 degree, and (f) azimuth 180 degree. The central frequencies at different azimuths are different from each other, which shows the anisotropy. Since for the central frequency estimation, we need to apply a certain length time window, the resolution of frequency results is a little low.

EDITED REFERENCES

Note: This reference list is a copyedited version of the reference list submitted by the author. Reference lists for the 2016 SEG Technical Program Expanded Abstracts have been copyedited so that references provided with the online metadata for each paper will achieve a high degree of linking to cited sources that appear on the Web.

REFERENCES

Carcione, J. M., 2000, A model for seismic velocity and attenuation in petroleum source rocks: Geophysics, **65**, 1080–1092, http://dx.doi.org/10.1190/1.1444801.

Chichinina, T. I., I. R. Obolentseva, G. Ronquillo-Jarillo, V. I. Sabinin, L. D. Gik, and B. A. Bobrov, 2007, Attenuation anisotropy of P- and S-waves: Theory and laboratory experiment: Journal of Seismic Exploration, **16**, 235–264.

Li, F.Y., S. Verma, H. Zhou, T. Zhao, and K. J. Marfurt, Seismic attenuation attributes with applications on conventional and unconventional reservoirs: Interpretation, **4**, SB63–SB77, http://dx.doi.org/10.1190/INT-2015-0105.1.

Lynn, H., and W. Beckham, 1998, P-wave azimuthal variations in attenuation, amplitude and velocity in 3D field data: Implications for mapping horizontal permeability anisotropy: 68th Annual International Meeting, SEG, Expanded Abstracts, 193–196, http://dx.doi.org/10.1190/1.1820318.

MacBeth, C., 1999, Azimuthal variation in *P*-wave signatures due to fluid flow: Geophysics, **64**, 1181–1192, http://dx.doi.org/10.1190/1.1444625.

Perez, R., 2009, Quantitative petrophysical characterization of the Barnett shale in Newark east field, Fort Worth Basin: M.S. thesis, University of Oklahoma.

Schoenberg, M., and J. Douma, 1988, Elastic wave propagation in media with parallel fractures and aligned cracks: Geophysical Prospecting, **36**, 571–590, http://dx.doi.org/10.1111/j.1365-2478.1988.tb02181.x.

Thompson, A. M., 2010, Induced fracture detection in the Barnett Shale FT. Worth Basin, Texas: M.S. thesis, University of Oklahoma.

Thomsen, L., 1986, Weak elastic anisotropy: Geophysics, **51**, 1954–1966, http://dx.doi.org/10.1190/1.1442051.